

Evidence of in-plane ferromagnetic order probed by planar Hall effect in the geometry-confined ruthenate $\text{Sr}_4\text{Ru}_3\text{O}_{10}$

Yan Liu,^{1,2} Jiyong Yang,^{1,*} Weike Wang,¹ Haifeng Du,¹ Wei Ning,¹ Langsheng Ling,¹ Wei Tong,¹ Zhe Qu,¹ Gang Cao,³ Yuheng Zhang,^{1,4} and Mingliang Tian^{1,4,5,†}

¹The Anhui Key Laboratory of Condensed Matter Physics at Extreme Conditions, High Magnetic Field Laboratory of the Chinese Academy of Science, Hefei 230031, Anhui, China

²University of Science and Technology of China, Hefei 230031, Anhui, China

³Department of Physics, University of Colorado at Boulder, Boulder, Colorado 80309, USA

⁴Collaborative Innovation Center of Advanced Microstructures, Nanjing University, Nanjing 210093, China

⁵Hefei Science Center, Chinese Academy of Sciences, Hefei 230031, Anhui, China

(Received 9 December 2016; revised manuscript received 21 February 2017; published 4 April 2017)

The magnetic structure in the strongly correlated ruthenate $\text{Sr}_4\text{Ru}_3\text{O}_{10}$ has been debated for a long time and still remains elusive. Here, we perform a systematically planar Hall effect study on a single-crystalline $\text{Sr}_4\text{Ru}_3\text{O}_{10}$ nanostripe with a thickness of less than 100 nm. Large sharp switching behavior is observed in the planar Hall resistance, unambiguously indicating a strong anisotropic in-plane ferromagnetic order in the nanostripe, which is in contrast to the bulk system. Temperature-dependent evolution of the in-plane magnetism reveals that the in-plane spin order transforms from a single-domain state below a Curie temperature T_C into a multidomain state below a critical temperature T_M , probably due to the inherent strong spin-orbit coupling driven reconfiguration of spins between the c axis and the ab plane.

DOI: [10.1103/PhysRevB.95.161103](https://doi.org/10.1103/PhysRevB.95.161103)

The $4d$ perovskite $\text{Sr}_{n+1}\text{Ru}_n\text{O}_{3n+1}$ family with strong inherent spin-orbit coupling exhibits rich and fascinating properties, such as spin-triplet superconductivity in single-layered Sr_2RuO_4 ($n = 1$) [1] and field-induced metamagnetic quantum criticality in double-layered $\text{Sr}_3\text{Ru}_2\text{O}_7$ ($n = 2$) [2]. In contrast, triple-layered $\text{Sr}_4\text{Ru}_3\text{O}_{10}$ ($n = 3$) [see Fig. 1(a)] shows a ferromagnetic (FM) transition at a Curie temperature of $T_C = 105$ K, followed by an additional magnetic transition at a temperature of $T_M \sim 50$ K [3,4]. Below T_M , its magnetism is strongly anisotropic, showing a FM ordering along the c axis but an antiferromagnetic (AFM)-like or paramagnetic character in the ab plane [3,4].

While several magnetic-field-induced exotic phenomena, including the metamagnetic transition [4,5], strong magnetoelastic coupling [6,7], and multiple ultrasharp magnetoresistance (MR) steps [8,9], were observed when sweeping the in-plane magnetic field below T_M , the physical mechanism still remains elusive. For example, the nature of the metamagnetic transition was assigned to be a magnetic-field-induced AFM or paramagnetic to a FM transition, as suggested by a Raman study [6], while transport measurements indicated that the metamagnetic transition is most likely a field-induced evolution of the low polarized (LP) and forced polarized ferromagnetic (FFM) domains [8–10]. Unfortunately, neither long-range AFM nor LP or FFM order in the ab plane were demonstrated by a recent neutron diffraction study [7], leading to confusion regarding the in-plane magnetic structures.

To understand the mysterious in-plane magnetic structures and uncover the puzzles of the exotic phenomena, here we performed systematically measurements of in-plane longitudinal and transverse magnetoresistance on geometrically confined

single-crystalline $\text{Sr}_4\text{Ru}_3\text{O}_{10}$ nanostripes with a lateral size of less than $10 \mu\text{m}$ and a thickness of less than 100 nm, which is on the order of most magnetic domains. Generally, transverse magnetoresistance (R_{xy}) with an in-plane magnetic field is also called the planar Hall effect (PHE), which is more sensitive to the orientation of the in-plane magnetic order than the longitudinal one (R_{xx}) [11]. We have observed a pronounced angular-dependent switching behavior on R_{xy} in the entire temperature range below T_C when sweeping magnetic fields in the ab plane. The switching amplitude was found to increase gradually until T_M , and then it decreased with continuously decreasing temperature, accompanied by the smoothness of the turn-on switching. These results provide clear evidence that there indeed exists an in-plane FM order with strong anisotropy in geometrically confined $\text{Sr}_4\text{Ru}_3\text{O}_{10}$. Based on the results of the evolution of the PHE with temperature, the longstanding issues concerning the in-plane exotic phenomena can be well understood. Both the additional magnetic transition at T_M and the metamagnetic transition are probably the results of the reconfiguration of the magnetic ordering between the c axis and the ab plane.

$\text{Sr}_4\text{Ru}_3\text{O}_{10}$ nanostripes were obtained by scotch-tape-based micromechanical exfoliation from a high-quality bulk single crystal grown by flux techniques [3]. The stripes with a lateral size of $\sim 10 \mu\text{m}$ were transferred to a silicon substrate covered with 300-nm-thick silicon dioxide on the top of the surface. Six terminal electrical contacts were made using the electron-beam lithography (EBL) technique, followed by deposition of Ti/Au (5 nm/100 nm) electrodes [Fig. 1(b)]. The schematic arrangement of the transport measurement is shown in Fig. 1(c), where the dc current I is injected along the x axis, i.e., the [100] direction, and the magnetic field H is applied in the x - y plane (i.e., the ab plane). The longitudinal and transverse resistances R_{xx} and R_{xy} were measured using a physical property measurement system (PPMS, Quantum Design).

*Author to whom correspondence should be addressed: jiyyang@hmf.ac.cn

†tianml@hmf.ac.cn

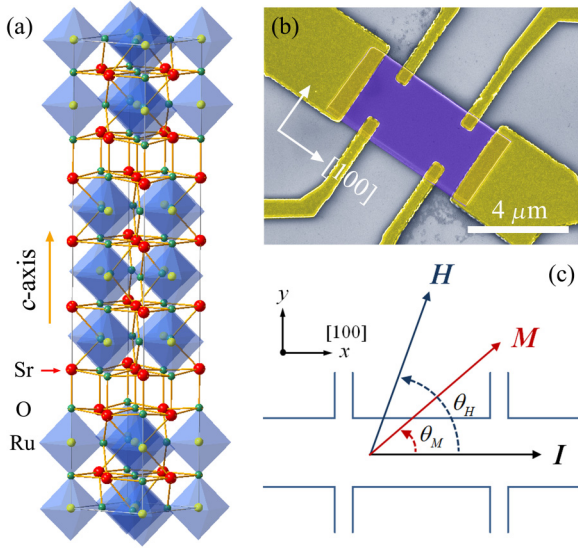


FIG. 1. (a) Crystal structure of $\text{Sr}_4\text{Ru}_3\text{O}_{10}$. (b) A scanning electron microscope image of a $\text{Sr}_4\text{Ru}_3\text{O}_{10}$ Hall bar device with thickness $d = 89$ nm. (c) Sketch of the relative orientations of the applied current I , the external field H , and the in-plane magnetization M in the transport measurement process. θ_M (θ_H) is the angle enclosed by I and M (I and H).

Figure 2(a) shows the temperature-dependent R_{xx} of two nanostripes with thicknesses $d = 34$ and 89 nm. Two anomalies, one at 105 K and the other around 25 K, are observed. The former one is caused by the FM transition, which is consistent with that of the bulk ($T_C \sim 105$ K) [12,13], while the latter anomaly, which is reasonably caused by an additional magnetic transition, is shifted to about 25 K, much lower than $T_M \sim 50$ K for the bulk [12–14]. The residual resistance ratio, $\text{RRR} = R_{xx}(300 \text{ K})/R_{xx}(2 \text{ K})$, for both samples reaches about 60, indicating the high quality of the thin crystals, where

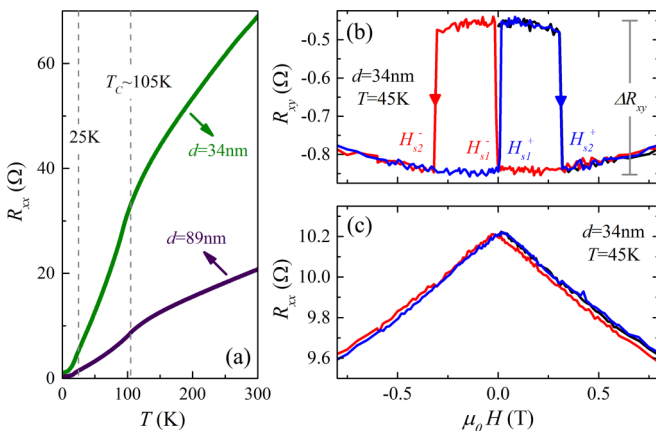


FIG. 2. (a) Temperature-dependent longitudinal resistance R_{xx} of $\text{Sr}_4\text{Ru}_3\text{O}_{10}$ nanostripes with different thicknesses d . (b) and (c) are, respectively, the in-plane magnetic-field-dependent R_{xy} and R_{xx} of a 34-nm-thick nanostripe at 45 K obtained by zero-field cooling. Arrows in (b) indicate the sweep direction of the field. H_{s1}^+ (H_{s1}^-) and H_{s2}^+ (H_{s2}^-) indicate, respectively, the switching field of the resistive jumps for an upward (downward) field sweep.

the residual resistivity at 2 K is $3.9 \mu\Omega \text{ cm}$ ($d = 34$ nm) and $3.04 \mu\Omega \text{ cm}$ ($d = 89$ nm), respectively.

Figures 2(b) and 2(c), respectively, show the field-dependent R_{xy} and R_{xx} obtained from a 34-nm-thick nanostripe with an in-plane magnetic field H aligned nearly along the direction of the current I (i.e., $[100]$ direction) at 45 K. The measurements were carried out in zero-field-cooling conditions from above 140 K ($>T_C$). The trace of the initial sweeping is labeled as black. When the field is swept down from above, the R_{xy} sharply switches up at the critical field H_{s1}^- and then switches down at H_{s2}^- , as shown in Fig. 2(b). Similar switching features also occur at H_{s1}^+ and H_{s2}^+ by sweeping the field up. The superscript + (–) indicates the up (down) sweeping direction of the field. It is seen that the magnitude ΔR_{xy} of the switching is as high as $\sim 0.4 \Omega$. In contrast, the corresponding R_{xx} presents a typical negative MR with increasing H [Fig. 2(c)], without a clear change in the resistance at the critical fields, indicating the switching behavior mainly happens in transverse resistance.

For a regular nonmagnetic metal or semiconductor, the Hall resistance in the ab plane originating from the deflection of the charge carriers by the Lorentz force can be obtained only when the magnetic field is normal to the plane. The giant switching phenomenon in R_{xy} with a field inside the ab plane is unusual for a metal, but is reminiscent of the so-called PHE reported previously in FM films with strong magnetic anisotropy, such as (Ga,Mn)As [15] and (La,Sr)MnO₃ [16]. In the FM sample, the transverse resistance R_{xy} , i.e., the planar Hall resistance, can be expressed as [11,17]

$$R_{xy} = \frac{k}{d} M^2 \sin 2\theta_M, \quad (1)$$

where M and d are, respectively, the in-plane magnetization and the thickness of the sample. θ_M is the angle between the direction of the current (I) and M [Fig. 1(c)] and k is a coefficient related to the anisotropic MR. Switching in R_{xy} can be observed if M is strongly anisotropic. In this case, M will present an abrupt change of its direction (i.e., angle θ_M) when the sweeping field H is applied noncollinearly with the easy axis of M . Therefore, the observation of planar Hall switching in the $\text{Sr}_4\text{Ru}_3\text{O}_{10}$ nanostripe provides direct evidence that a FM order must exist with strong anisotropy in the ab plane.

To clarify this issue, we have detected the field angle θ_H dependent property of R_{xy} under various intensities of the magnetic field. Figure 3(a) shows the R_{xy} - θ_H curves under different magnetic fields at 45 K in the 89-nm-thick sample, where θ_H is the angle between the in-plane field H and the current I . Based on Eq. (1), a “sinusoidal-shaped” twofold symmetry should be expected in the R_{xy} - θ_H relation if the applied in-plane magnetic field H is higher than the saturation field (i.e., $\theta_M \sim \theta_H$). Indeed, as shown in Fig. 3(a), the expected symmetry with four extremes at $\theta_H = 45^\circ$, 135° , 225° , and 315° is well confirmed at $H = 2$ T. Meanwhile, as the intensity of H decreases, the R_{xy} - θ_H curves gradually change into a “square-wave” form with twofold symmetry, accompanied by clear hysteresis below 0.3 T near all $\langle 100 \rangle$ directions, indicating that the magnetic polarization no longer linearly follows the external field H . These results suggest

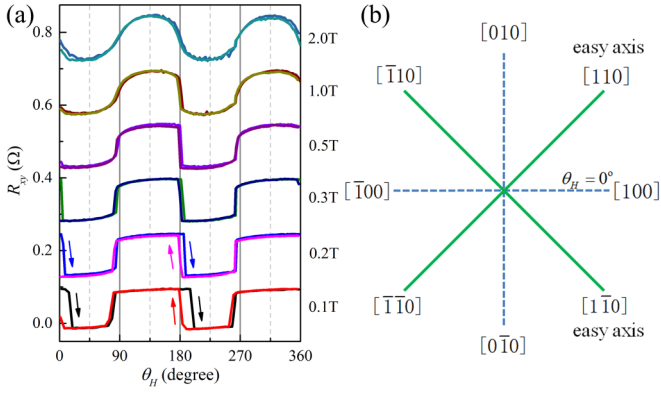


FIG. 3. (a) R_{xy} - θ_H curves measured at different in-plane magnetic fields from the 89-nm-thick nanostructure at 45 K. The curves have been shifted vertically for clarity. (b) Schematic diagram for illustrating the in-plane magnetic anisotropy of $\text{Sr}_4\text{Ru}_3\text{O}_{10}$.

that an in-plane FM order with strong magnetic anisotropy does exist in geometrically confined $\text{Sr}_4\text{Ru}_3\text{O}_{10}$. Based on the facts that (i) R_{xy} always remains at a low (or high) resistance state with a magnitude constant of $\theta_H = 45^\circ$ (or 135°) for $H < 0.3$ T, and (ii) the hysteresis near $[100]$ (or $[\bar{1}00]$) is wider than that near $[010]$ (or $[0\bar{1}0]$), we can obviously conclude that the in-plane magnetic anisotropy is nearly cubic, and the $\langle 110 \rangle$ direction (i.e., 45° or 135°) is the easy axis of the magnetization in the ab plane. The switching behavior in PHE

shown in Fig. 2(b) is thus a result of the flop of the in-plane magnetization between the $[\bar{1}10]$ and $[110]$ directions induced by sweeping the magnetic fields, as schematically shown in Fig. 3(b). The sharpness of the switching at H_{s1}^+ (H_{s1}^-) and H_{s2}^+ (H_{s2}^-) indicates clearly the single-domain nature in the nanostructure.

In $\text{Sr}_4\text{Ru}_3\text{O}_{10}$ bulk, both the magnetization and neutron diffraction measurements have found that the Ru moments are primarily FM arranged along the c axis at the ground state [3,4,7]. The observation of the in-plane FM order must be the result of the confined geometry, where the reduction of the thickness in $\text{Sr}_4\text{Ru}_3\text{O}_{10}$ favors the Ru moments aligned from the c axis to the ab plane. Therefore, the occurrence of in-plane FM order allows us to detect the in-plane magnetic behavior at various temperatures using the PHE measurement.

Figure 4 shows the $R_{xx}(H)$ and $R_{yy}(H)$ characteristics at different temperatures from the 34- and 89-nm-thick samples with H aligned near the direction of the applied current. As T decreases, the R_{xx} presents negative MR with increasing H until about 25 K, then a positive MR appears in the low field range for $T < 25$ K [Figs. 4(a) and 4(c)]. Such a contrast in MR behavior near 25 K implies that the magnetic scattering mechanism could change dramatically at this temperature, which is consistent with the additionally resistive anomaly at $T_M \sim 25$ K in the R - T curve, as shown in Fig. 2(a). However, it is worth noting that, from Figs. 4(b) and 4(d), the resistive jump in R_{xy} exists robustly in the whole temperature

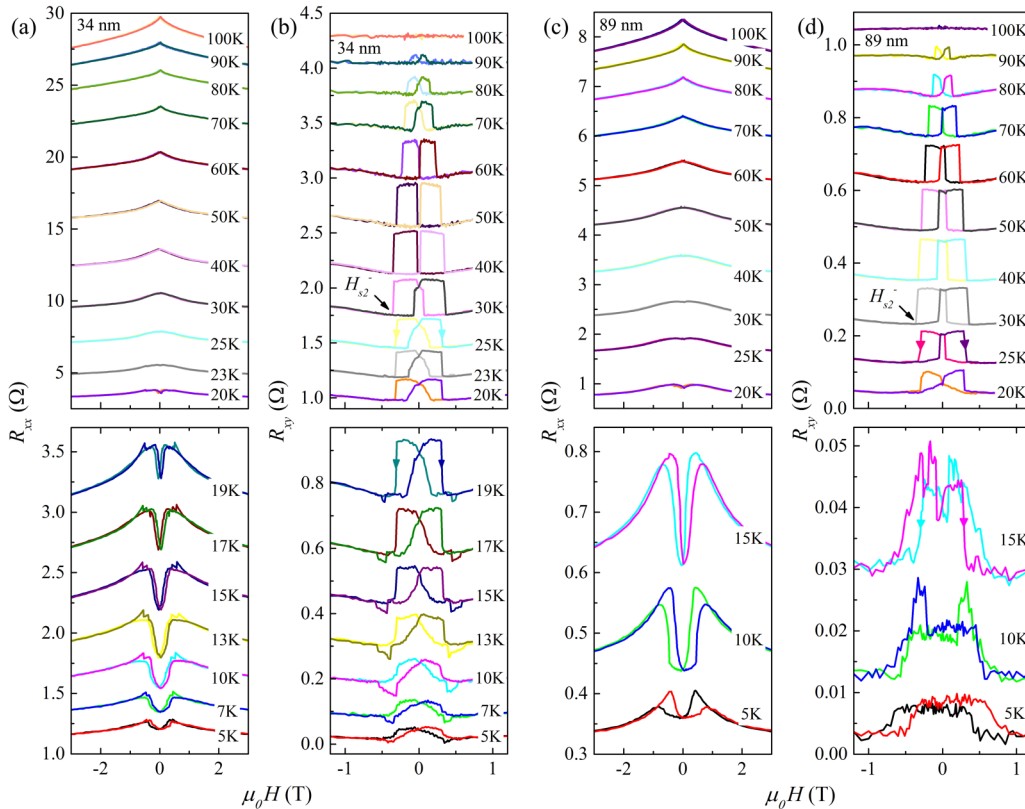


FIG. 4. R_{xx} - H and R_{yy} - H curves of $\text{Sr}_4\text{Ru}_3\text{O}_{10}$ nanostructures at different temperatures with H applied almost parallel to the current I . (a) and (b) are for the 34-nm-thick nanostructure, and (c) and (d) are for the 89-nm-thick nanostructure, respectively. The curves have been shifted vertically for clarity. Note that the vertical scale bar of the bottom panels has been rescaled.

range below T_C , indicating the in-plane FM order remains even at temperatures below $T_M \sim 25$ K in the $\text{Sr}_4\text{Ru}_3\text{O}_{10}$ nanostripe.

When carefully checking the switching property of the R_{xy} , one prominent signature is that the turn-on switching at H_{s1}^+ (H_{s1}^-) is no longer sharp below about 25 K in both nanostripes, but the turn-off switching at H_{s2}^+ (H_{s2}^-) remains sharp until the temperature is down to 15 K in the 34-nm-thick sample while it is blurred in the 89-nm-thick sample. Below 15 K, the switching becomes very weak and is no longer sharp. As mentioned above, the sharp switching behavior in the PHE is an indication of single-domain magnetic order. Therefore, the smoothness of the switching below 25 K implies that the evolution of the domain structures in the ab plane will, in turn, take transformations from a single-domain FM state at $T > 25$ K to a less ordered multidomain state below 25 K, and it seems to be easier to form a multidomain state in the thicker sample. In other words, the magnetic order in the ab plane is intrinsically weakened below T_M (~ 25 K) even if the thermal fluctuation has been reduced. This assignment is also partially justified by the facts that (i) the switching height ΔR_{xy} [proportional to kM^2 ; see Eq. (1)] is reduced at low temperatures (note that the vertical scale bar of the bottom panels of Fig. 4 has been rescaled), and (ii) additional tiny resistive jumps gradually emerge below 20 K.

Because the anomaly in resistance at T_M and the weakness of magnetization below T_M can be also seen in bulk systems [3,4,9], the similarity allows us to conclude that they must share the same origin. It has been theoretically proposed that the expansion of the c axis (or ab axis) favors the Ru moments aligned along the c direction (or ab plane) due to inherently strong spin-orbit coupling [18]. Indeed, the negative thermal expansion along the c axis below T_M was verified by a neutron diffraction study in $\text{Sr}_4\text{Ru}_3\text{O}_{10}$ [7]. Hence, a possible mechanism for the weakness of magnetization is that the spin-orbit coupling drives the rearrangement of spins from the ab plane slightly to the out of plane, and thus leads to a multidomain FM structure in the ab plane due to the canted magnetization below T_M . Because the main

difference between the nanostripe and the bulk is the size confinement, this evolution of the spins is able to understand the in-plane metamagnetic transition in the bulk, though there is no evidence of such metamagnetic behavior in the nanostripe. The in-plane metamagnetic transition observed in the bulk below T_M is essentially a field-induced rearrangement of moments from the c axis to the ab plane, which is affected significantly by the size effect.

We would like to point out that our result obtained in the confined geometry may provide insight on the nature of exotic phenomena in $\text{Sr}_4\text{Ru}_3\text{O}_{10}$, such as the second magnetic transition [3,4] and strong magnetoelastic coupling [6]. All these exotic phenomena actually originate from the spin-orbit coupling driven reconfiguration of spins. The significant decrease of T_M to 25 K (bulk ~ 50 K) in our high-quality nanostripe might be the competition between the size confinement introduced spin reorientation energy and the spin-orbit coupling generated spin reconfiguration energy, where the former forces the spins aligned in the ab plane while the latter drives the spins arranged out of plane. Hence, the in-plane magnetic moments in the bulk are always less ordered below $T_M \sim 50$ K due to the lack of a size effect.

In summary, we have found an in-plane FM order with strong anisotropy induced by reducing the thickness of $\text{Sr}_4\text{Ru}_3\text{O}_{10}$. The evolution of the magnetization with temperatures is the result of reorientation of the magnetic moments from a single-domain structure to a multidomain state. The inherent strong spin-orbit coupling driven reconfiguration of spins between the c axis and the ab plane essentially may be the cause of the observed exotic phenomena in $\text{Sr}_4\text{Ru}_3\text{O}_{10}$.

This work was supported by the National Natural Science Foundation of China (Grants No. 11674323, No. U1432251, No. 11374302, No. U1532153, No. U1332209, No. 11474290, and No. 11304319), and the program of Users with Excellence, the Hefei Science Center of CAS, and the CAS/SAFEA international partnership program for creative research teams of China.

-
- [1] K. Ishida, H. Mukuda, Y. Kitaoka, K. Asayama, Z. Q. Mao, Y. Mori, and Y. Maeno, *Nature (London)* **396**, 658 (1998).
- [2] S. A. Grigera, P. Gegenwart, R. A. Borzi, F. Weickert, A. J. Schofield, R. S. Perry, T. Tayama, T. Sakakibara, Y. Maeno, A. G. Green, and A. P. Mackenzie, *Science* **306**, 1154 (2004).
- [3] M. K. Crawford, R. L. Harlow, W. Marshall, Z. Li, G. Cao, R. L. Lindstrom, Q. Huang, and J. W. Lynn, *Phys. Rev. B* **65**, 214412 (2002).
- [4] G. Cao, L. Balicas, W. H. Song, Y. P. Sun, Y. Xin, V. A. Bondarenko, J. W. Brill, S. Parkin, and X. N. Lin, *Phys. Rev. B* **68**, 174409 (2003).
- [5] E. Carleschi, B. P. Doyle, R. Fittipaldi, V. Granata, A. M. Strydom, M. Cuoco, and A. Vecchione, *Phys. Rev. B* **90**, 205120 (2014).
- [6] R. Gupta, M. Kim, H. Barath, S. L. Cooper, and G. Cao, *Phys. Rev. Lett.* **96**, 067004 (2006).
- [7] V. Granata, L. Capogna, M. Reehuis, R. Fittipaldi, B. Ouladdiaf, S. Pace, M. Cuoco, and A. Vecchione, *J. Phys.: Condens. Matter* **25**, 056004 (2013).
- [8] Z. Q. Mao, M. Zhou, J. Hooper, V. Golub, and C. J. O'Connor, *Phys. Rev. Lett.* **96**, 077205 (2006).
- [9] D. Fobes, M. H. Yu, M. Zhou, J. Hooper, C. J. O'Connor, M. Rosario, and Z. Q. Mao, *Phys. Rev. B* **75**, 094429 (2007).
- [10] Y. Nakajima, Y. Matsumoto, D. Fobes, M. Zhou, Z. Q. Mao, and T. Tamegai, *J. Phys.: Conf. Ser.* **150**, 042134 (2009).
- [11] K. Okamoto, *J. Magn. Magn. Mater.* **35**, 353 (1983).
- [12] Z. A. Xu, X. F. Xu, R. S. Freitas, Z. Y. Long, M. Zhou, D. Fobes, M. H. Fang, P. Schiffer, Z. Q. Mao, and Y. Liu, *Phys. Rev. B* **76**, 094405 (2007).
- [13] C. Mirri, F. M. Vitucci, P. Di Pietro, S. Lupi, R. Fittipaldi, V. Granata, A. Vecchione, U. Schade, and P. Calvani, *Phys. Rev. B* **85**, 235124 (2012).

- [14] Y. Liu, J. Y. Yang, W. K. Wang, H. F. Du, W. Ning, L. S. Ling, W. Tong, Z. Qu, Z. R. Yang, M. L. Tian, G. Cao, and Y. H. Zhang, *New J. Phys.* **18**, 053019 (2016).
- [15] H. X. Tang, R. K. Kawakami, D. D. Awschalom, and M. L. Roukes, *Phys. Rev. Lett.* **90**, 107201 (2003).
- [16] Y. Bason, L. Klein, J. B. Yan, X. Hong, and C. H. Ahn, *Appl. Phys. Lett.* **84**, 2593 (2004).
- [17] A. M. Nazmul, H. T. Lin, S. N. Tran, S. Ohya, and M. Tanaka, *Phys. Rev. B* **77**, 155203 (2008).
- [18] M. Cuoco, F. Forte, and C. Noce, *Phys. Rev. B* **73**, 094428 (2006).